Available online at www.sciencedirect.com

ScienceDirect

Physics of Life Reviews 31 (2019) 240–256

PHYSICS of LIFE reviews

www.elsevier.com/locate/plrev

Review

Spectral peculiarity and criticality of a human connectome

N. Pospelov [a], S. Nechaev [b,c,*], K. Anokhin [a,d], O. Valba [e,f], V. Avetisov [e], A. Gorsky [g,h]

[a] *Lomonosov Moscow State University, 119991, Moscow, Russia*
[b] *Interdisciplinary Scientific Center Poncelet (CNRS UMI 2615), 119002 Moscow, Russia*
[c] *P.N. Lebedev Physical Institute RAS, Moscow, Russia*
[d] *National Research Center "Kurchatov Institute", 123098, Moscow, Russia*
[e] *N.N. Semenov Institute of Chemical Physics RAS, 119991 Moscow, Russia*
[f] *Department of Applied Mathematics, National Research University Higher School of Economics, 101000 Moscow, Russia*
[g] *Institute for Information Transmission Problems RAS, 127051 Moscow, Russia*
[h] *Moscow Institute of Physics and Technology, Dolgoprudny, 141700 Russia*

Received 17 March 2019; accepted 6 July 2019
Available online 16 July 2019
Communicated by Felix Schoeller

Abstract

We have performed the comparative spectral analysis of structural connectomes for various organisms using open-access data. Our results indicate new peculiar features of connectomes of higher organisms. We found that the spectral density of adjacency matrices of human connectome has maximal deviation from the one of randomized network, compared to other organisms. Considering the network evolution induced by the preference of 3-cycles formation, we discovered that for macaque and human connectomes the evolution with the conservation of *local clusterization* is crucial, while for primitive organisms the conservation of *averaged clusterization* is sufficient. Investigating for the first time the level spacing distribution of the spectrum of human connectome Laplacian matrix, we explicitly demonstrate that the spectral statistics corresponds to the critical regime, which is hybrid of Wigner-Dyson and Poisson distributions. This observation provides strong support for debated statement of the brain criticality.

Keywords: Connectome; Spectral density; Level spacing; Criticality

1. Introduction

Understanding basic mechanisms of brain functioning in terms of the structure of underlying anatomical and functional neural networks is a challenging interdisciplinary issue which worries researchers over the decades. A current state of comprehensive studies of structural and functional neural connectivity networks (connectomes) can be found in [3,4,1,2]. To summarize the mainstream directions of modern research, one can highlight two questions of primary interest: (i) Which properties of the connectome are of key importance for an effective brain functioning at the cogni-

* Corresponding author at: Interdisciplinary Scientific Center Poncelet (CNRS UMI 2615), 119002 Moscow, Russia.
E-mail address: serguei.nechaev@u-psud.fr (S. Nechaev).

https://doi.org/10.1016/j.plrev.2019.07.003
1571-0645/

tive level and information processing? (ii) What are the operational mechanisms of the structural network evolution, allowing to arrive at a present pattern of the connectome organization?

These challenging questions spurred an avalanche of studies ranging from the investigation of the complete network of connections among the 302 neurons of the nematode Caenorhabditis elegans (C. elegans) [5] to the analysis of complex mammalian brain networks including the rat, cat, macaque and the human connectomes [3,7–9,6]. The initial analysis of the C. elegans data has led to a conjecture that from the topological point of view, the connectome is an example of a "small world" network with a high clusterization and "short path" structure [10]. Such a topological network lies between regular and completely random (Erdős-Rényi) topological graphs [11–13]. It was suggested that high clustering coefficient determines efficiency of inter-module brain processes, while small average path length provides an optimal embedding of large regions into a high-performance network, thus allowing to connect system processes on various scales. The small-world model fits well the properties of brain networks that combine high local connectivity with global information transmission. It links processing of neural information on local and global levels with peculiar properties of the brain network architecture.

Such a line of reasoning was developed in [14] where the connectome is identified with the scale-free network (see also [6]). Scale-free networks are characterized by a power-law vertex degree distribution, where the majority of nodes have few links, but a small number of hubs have a large number of connections, thus ensuring a high level of global network connectivity [15]. Both small-world and scale-free architectures are considered to be attractive candidates for efficient flow and integration of information in the network [16–18].

The hypothesis that brain networks exhibit scale-free topology became popular at the turn of the millennium, while nowadays there are many evidences that connectomes on various anatomical scales deviate from networks with the scale-free features. For example, it has been recognized that some properties of the connectome, such as, for example, the hierarchical structure, cannot be explained neither by the "small world" paradigm, nor in the frameworks of the scale-free concept. The emerging viewpoint is that the connectome realizes a new type of a network architecture.

To unravel specific organizational principles of the connectome, the comparative analysis of connectomes of different organisms [19] is of extreme importance. It provides hints for the identification of key structural properties of the neuronal network, crucial for the integrative functions across a variety of specific neuroanatomical organizations. Below we summarize major statistical and dynamic properties of connectomes of various organisms based of open-sources data analysis. Firstly, connectomes have typically a large modularity. Recall that the modularity measures the clusterization of the network and reflects its hierarchical structure [29–31]. The large modularity is confirmed in [32] by the high-resolution analysis of adjacency matrices of human connectomes for $N > 5 \times 10^4$ nodes. Secondly, structural connectomes have the "short path" property typical for the small-world networks. Thirdly, the signal spreading in connectomes demonstrates the synchronization [33–35].

Since any global brain function is a synergetic collective effect of many particular functions, it should be treated by appropriate methods capable to catch collective properties of underlying structural network. From this point of view, the comparative investigation of different connectomes undertaken in [20] via the analysis of their spectral properties, seems particularly promising (see also [22]). In our work we continue this line of reasoning and develop the comparative spectral approach.

Classical methods of the theory of complex networks are now widely used in neurobiology [3,4,1]. However, many commonly used characteristics, such as "betweenness centrality", "efficiency", and others reflect rather the properties of individual nodes of the network, than on the features of the network as a whole. In this work our attention is paid to the global properties of the connectome. For these purposes, the methods of spectral graph theory are well suited. The main objects of interest are the eigenvalues and eigenvectors of the matrices characterizing a graph, for example, adjacency and/or Laplace matrices. The spectrum of adjacency matrix (i.e. a set of eigenvalues) is an identifier of the network, its "fingerprint". Knowing the whole set of eigenvalues and eigenvectors, it is possible to restore the original network (with relatively rare exceptions, known as "isospectral graphs"). In the process of spectral decomposition, matrix elements of the network mix in a complex way, creating a "global" portrait of the network. For example, in the case of a graph represented as a Laplace matrix, the eigenvalues have a clear physical meaning: they represent the eigenfrequencies at which the spring-made graph resonates.

Much information concerning the structural properties of the connectome is stored in the spectral properties of adjacency and Laplacian matrices. The spectral density (distribution of eigenvalues) of the normalized Laplacian matrix of the connectome of C. elegans consists of the triangle-shaped "continuum" zone accompanied by several

low-energy isolated eigenvalues [20]. Such a shape of the spectral density is different from the one of the random Erdos-Renyi random graph, which has the semicircular-shaped normalized Laplacian spectrum of the main zone. The low-lying eigenvalues and corresponding eigenfunctions of the Laplacian matrix of the network carry the information about the transport properties. In particular, recently it has been found (see [36]) that the second eigenvalue, λ_2, is responsible for the diffusion of the signal between two hemispheres. The third eigenvalue, λ_3, seems to measure the radial diffusion in the connectome from the inner to outer regions [36]. The largest eigenvalue of the connectome Laplacian matrix does not deviate much from the eigenvalue typical for a purely random network with the same averaged characteristics, which means that the connectome typically does not develop the bipartite structure.

In our work we use networks from open sources: the objects of interest are Caenorhabditis elegans, Ciona intestinalis, macaque and human structural connectomes. We demonstrate that various structural and spectral properties of connectomes of different organisms can be designed in an "artificial evolution" (rewiring) of the network under specific constraints starting from the "null state" which is a randomized version of an initial network.

In our work we tackle in details spectral properties of experimentally available adjacency and Laplacian matrices of structural networks. The simplest characteristics of the spectrum is the distribution of eigenvalues, known as the spectral density. However, more refined characteristics like the statistical correlators of the spectral densities, carry an additional information about the network properties. The investigation of the "level spacing distribution" (i.e. the distribution of distances between the neighboring eigenvalues) allows one to identify the eigenvalue ("level") statistics using the standard methods of the spectral analysis. The "level spacing" distribution provides the information concerning the localization properties (the propagation of the excitation) in the connectome. To the best of our knowledge, the spectral statistics has not yet been discussed in the context of the structural connectome.

Our findings are as follows:

- The spectral density of adjacency matrices of human structural connectomes has the maximal deviation from the spectral density of the randomized (via the Maslov-Sneppen procedure) network compared to other organisms.
- The spectral density of adjacency matrices of structural connectomes for primitive organisms (C. elegans and C. intestinalis) can be reproduced by conserving the vertex degree in all nodes of randomly rewired network under the control of the averaged number of 3-cycles in the stochastically evolving network.
- The spectral density of adjacency matrices of structural connectomes of higher organisms (macaque and human) can be reproduced by random rewiring of network's links if besides the conservation of the vertex degree, we demand also the conservation of the detailed local graph connectivity.
- The level spacing distribution for structural human connectomes corresponds to the critical regime, which is the hybrid of Wigner-Dyson and Poisson level statistics.

2. Results

2.1. Spectral analysis of structural connectomes

We have compared spectral densities (distribution of eigenvalues) of adjacency matrices of structural connectomes of various organisms with their randomized "null states" obtained via the Maslov-Sneppen procedure (see Methods). Our numeric analysis presented in Fig. 1 and Fig. 2 allows to conclude that the "null state" network with conserved vertex degrees in all nodes, reproduces with a good accuracy the spectrum of the experimental connectome adjacency matrix of C. elegans and C. intestinalis, but not of macaque and human.

The vertex degree conservation is a candidate for a "sufficient" minimal set of conservation laws which control the evolution of these organisms. Conserving (in addition to the vertex degrees) the mean number of triangles in the network (the "first level" triangle preserving algorithm, TPC), we improve the spectral coincidence between initial network and its randomized version for primitive organisms (C. elegans and C. intestinalis) – see Fig. 1.

The more refined procedure consisting of the conservation of the local clustering coefficient for all nodes of the network (the "second level" local clustering constraint, LCC) leads to a significant improvement of coincidence between initial spectral density and its randomized version for higher organisms (macaque and human) – see Fig. 2.

The quantitative characteristics of the difference between spectral densities is expressed in terms of the "earth mover's distance" (EMD) [37,39] between the spectral density of the actual network and its randomized version, under the condition of vertex degree conservation in all graph nodes. In Table 1 we have compared the earth mover's

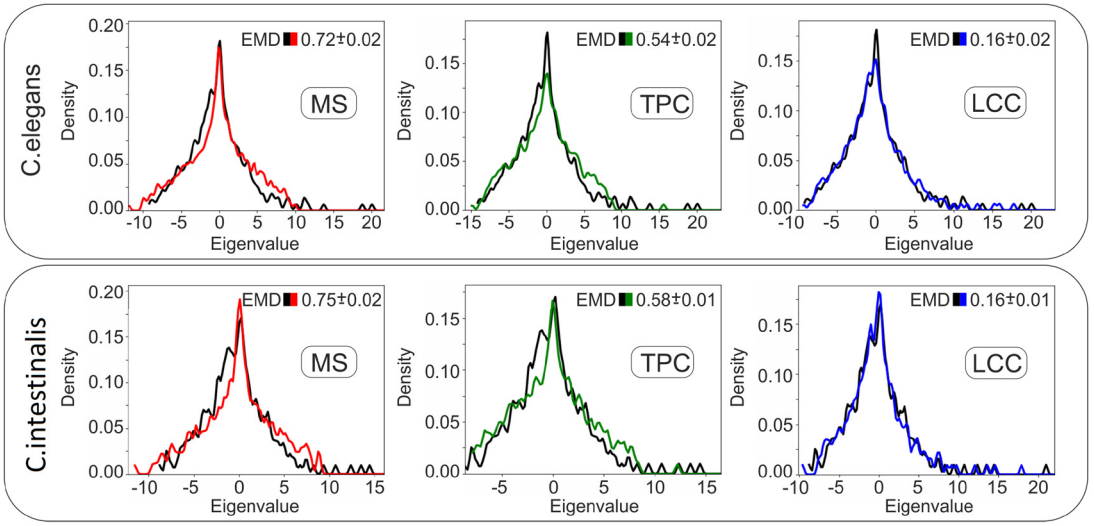

Fig. 1. Spectral densities of adjacency matrices of animal connectomes along with the MS-randomized version (red), the TPC-randomized version (green) and the LCC-randomized version (blue). First panel – C. elegans, second panel – C. intestinalis. The definitions of abbreviations: MS = Maslov-Sneppen, TPC = triangle preserving constraint ("first level" evolutionary algorithm), LCC = local clustering constraint ("second level" evolutionary algorithm).

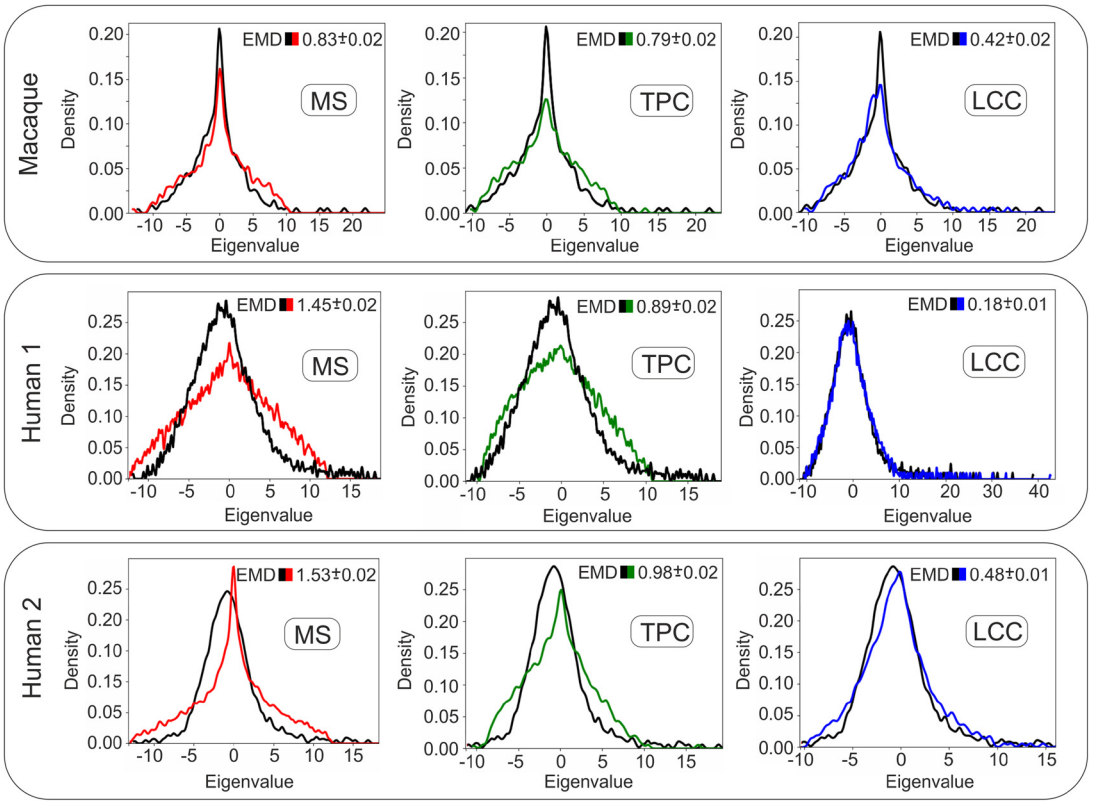

Fig. 2. Spectra of adjacency matrices of a human and macaque connectome along with its MS-randomized version (red), TPC-randomized version (green) and LCC-randomized version (blue) Human 1: data from Hagmann et al. [21]; Human 2: data from Open Connectome Project [25]; MS = Maslov-Sneppen, TPC = triangle preserving constraint ("first level" evolutionary algorithm), LCC = local clustering constraint ("second level" evolutionary algorithm).

Table 1
Comparative analysis of animals by their earth mover's distance (EMD) from Maslov-Sneppen (MS) randomized "null state" network – second column, the EMD from initial network and the network obtained by triangle preserving constraint (TPC) – third column, and by local clustering constraint (LCC) – fourth column.

Organism	EMD from MS	EMD from TPC	EMD from LCC
C. elegans	$E_{Ce} = 0.72 \pm 0.02$	$E_{Ce} = 0.54 \pm 0.02$	$E_{Ce} = 0.16 \pm 0.02$
C. intest.	$E_{Ci} = 0.75 \pm 0.02$	$E_{Ci} = 0.58 \pm 0.01$	$E_{Ci} = 0.16 \pm 0.01$
Macaque	$E_{M} = 0.83 \pm 0.02$	$E_{M} = 0.79 \pm 0.02$	$E_{M} = 0.42 \pm 0.02$
Human 1	$E_{H1} = 1.45 \pm 0.02$	$E_{H1} = 0.89 \pm 0.02$	$E_{H1} = 0.18 \pm 0.01$
Human 2	$E_{H2} = 1.53 \pm 0.02$	$E_{H2} = 0.98 \pm 0.02$	$E_{H2} = 0.48 \pm 0.02$

distances for spectral distributions of connectomes of all organisms (C. elegans, C. intestinalis, macaque and human) from: (i) the Maslov-Sneppen random "null state" (second column), (ii) the network optimized by the triangle preserving constraint, (iii) the network optimized by the local clustering constraint.

The results presented in Table 1 demonstrate that the human connectome is much "farther" from the MS-randomized "null state" than the brain networks of other animals. One could speculate that such a difference is a consequence of the evolutionary selection in the neuronal network in nature (see Discussion for more details). First level triangle preserving clustering (TPC) essentially decreases EMD of C. elegans and Ciona, but not of macaque and human. The spectral distance of macaque and human connectomes from their TPC-randomized versions are still essential, indicating that preserving mean clustering is not sufficient to reproduce the network properties for higher organisms.

To test whether the stated results are not the artifacts of the network size (the two considered human connectomes have about 1000 and 600 nodes respectively, while networks of other animals have less than 300 vertices), we have performed numerical simulations on smaller human brain networks. From the experimental data taken from the Open Connectome Project we took networks of various sizes (from 250 to 6000 nodes) and found that the difference in the spectral distance is insensitive to the network size. We have also carried out simulations with the data on human connectomes taken from other sources (the data available at UMCD database [26]) to exclude the possibility that our results are the artifacts of algorithms used in the data processing of OCP database. We found that the effect of increasing the spectral distance for humans with respect to other animals is supported, which we consider as an indirect confirmation of its generality.

2.2. *Impact of local clustering on the network spectrum*

The peculiarities of the network dynamics for higher organisms prompted us to suggest an existence of N additional "conservation laws" consisting in preservation of *local clustering* for each network node. The local clustering has been used in the analysis of generic exponential graphs (see, for instance [28]), however in the context of the connectome, it has been applied for the C. elegans only in rather restricted context.

We have mentioned that the evolution of a connectome of higher organisms is apparently much more complex process compared to the evolution of primitive organisms. To try to restore back the spectrum of macaque or human network from its Maslov-Sneppen randomized "null state", we need to impose much more constraints on available network rewiring. The imposed "second level" constraints preserving the local clustering permit to reduce for macaque and human the EMD between the actual network structure and its randomized version. Some properties of graphs with such a set of local constraints were discussed in [28].

Among the network's characteristics affecting its spectrum, the number of triangles, T_i involving a given node, i ($i = 1, \ldots, N$), is of much importance. The impact of the local clustering coefficient associated with a given node i, is crucial. The coincidence of spectral densities between structural network of higher organisms and their MS-randomized version exposed to artificial evolutionary process, could not be achieved by preserving only the *average* clustering of the total number of triangles, $\langle T \rangle = \frac{1}{N} \sum_{i=1}^{N} T_i$. Instead, the full vector $\mathbf{T} = \{T_1, \ldots, T_N\}$ should be conserved. Conserving N additional quantities, $\{T_1, \ldots, T_N\}$, (for all network nodes), one can significantly improve the coincidence of the spectra of a pattern and its MS-randomized networks for macaque and human structural connectomes in terms of the earth mover's distance, as it is shown in Fig. 2. This result is stable for all connectome

samples under investigation and for networks of various sizes. Such a feature demonstrates the important role of local clustering in the structure of brain networks.

Similar set of conservation laws has been proposed for the analysis of real networks in [28]. For the connectome of the C. elegans it was argued that tuning the single parameter which controls the local connectivity, it is possible to fit well the spectral density. Our study provides further evidence of the importance of various conservation laws in the evolution of connectomes including human connectomes.

2.3. Criticality of the human connectome

Let $A = \{a_{ij}\}$ be the adjacency matrix of an undirected network with matrix elements $a_{ij} = a_{ji}$ taking binary values: $a_{ij} = 1$, if nodes i and $j \neq i$ are connected, and $a_{ij} = 0$ otherwise. The absence of self-connections means that the diagonal elements vanish, i.e. $a_{ii} = 0$. At length of the current work, we have studied spectral properties of adjacency matrices of networks, however in many papers another characteristic, the Laplacian of the graph, is under the investigation. The Laplacian matrix, $\mathcal{L}$, of a network is, by definition,

$$\mathcal{L} = D - A \tag{1}$$

where D is the degree matrix of the network, The elements of D are: $d_{ij} = \deg(v_i)$ if $i = j$ and $d_{ij} = 0$ otherwise, where $\deg(v_i)$ is the degree of the vertex i. All eigenvalues, λ_n ($n = 1, \ldots, N$) of the Laplacian $\mathcal{L}$ are real. For regular graphs (i.e. for graphs with constant vertex degree) the spectra of A and $\mathcal{L}$ are connected by a linear transform.

The spectrum of $\mathcal{L}$ is positive with the minimal eigenvalue $\lambda_1 = 0$. From the graph theory it is known that the multiplicity of λ_1 equals to the number of disconnected components in the network. This fits with the identification of the number of separated discrete modes as of the number of clusters. Indeed, when some isolated eigenvalue hits zero, the cluster becomes disconnected from the rest of the network. The second eigenvalue, λ_2, carries the essential topological information, known as the "algebraic network connectivity", which measures the minimal number of links to be cut to get disconnected parts of the network. The value of λ_2 plays an important role in network relaxational and transport properties, and defines the inverse diffusion time. Also, λ_2 plays a crucial role in determining synchronization of multiplex (multilayer) networks [40]. The corresponding eigenvector (the so-called "Fiedler vector") sets the bijection between the network layers.

One of the most informative characteristics, which delivers the information about the localization properties of excitations on the network, is the so-called "level spacing" distribution, $P(s)$, where s is the normalized distance between nearest-neighboring eigenvalues of the Laplacian matrix of the network. It is known from the theory of random matrices (see, for example, [41]) that if $P(s)$ shares the Wigner-Dyson level statistics if the excitations are delocalized, while if $P(s)$ is exponential if the Poisson-distributed excitations are localized and the system behaves as an insulator:

$$P(s) \sim \begin{cases} s e^{-s^2/\sigma^2} & \text{Wigner surmise (delocalized behavior)} \\ e^{-s/\delta} & \text{Poissonian statistics of events (localized behavior)} \end{cases} \tag{2}$$

where σ, δ are some positive constants, and $s = \frac{\lambda_i - \lambda_{i+1}}{\Delta}$ is the normalized (by the spectral interval Δ) distance between nearest-neighboring eigenvalues.

However, there is the third critical regime for $P(s)$ which occurs when some control parameter is tuned such that the system stays exactly at the point of the phase transition. In this case the function $P(s)$ is the hybrid of Wigner-Dyson and Poisson statistics at all energies. At small values of s it shares the Wigner surmise, while the large-s tail follows the Poisson law [42]. Such a hybrid statistics serves as the spectral benchmark of the criticality in the system and is widely used in condensed matter physics.

We have used a standard procedure to construct the level spacing: selecting a certain spectral region, Δ, we computed a set of gaps between sequential eigenvalues and averaged them over Δ. Finally, we presented the distribution of gaps between adjacent eigenvalues (in relative units) in coordinates (x, y), which allows for straightforward identification of the spectral statistics by the slope of the curve: for x-axis we chose $\log s$, while for y-axis we take the function $L(s)$, defined as follows

$$L(s) = \log\big(-\log(1 - C(s))\big); \qquad C(s) = \int_{-\infty}^{s} P(s')ds' \tag{3}$$

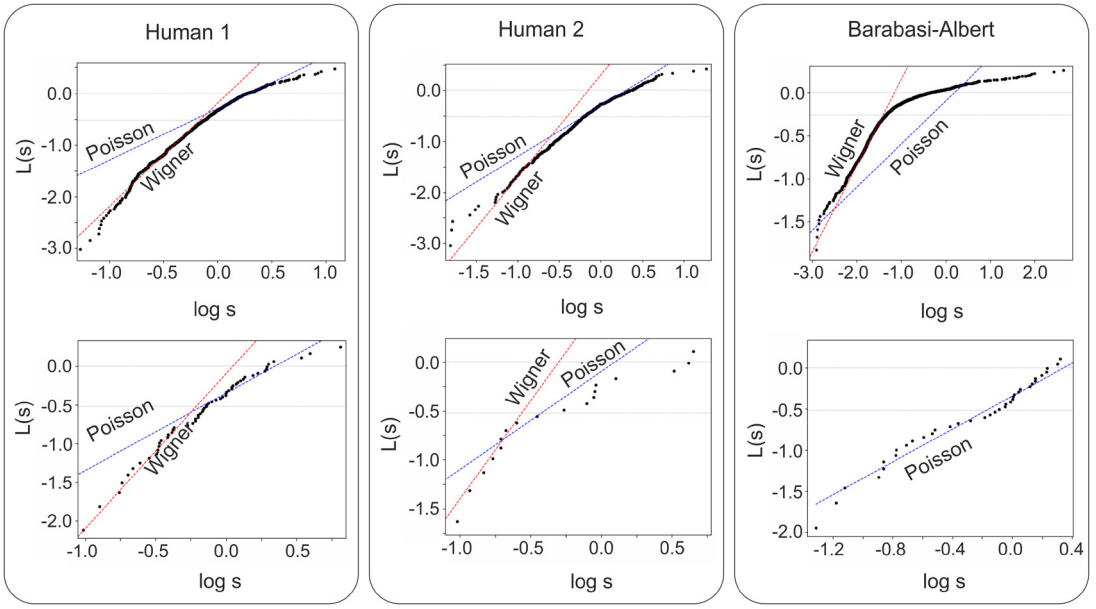

Fig. 3. Level spacings of the Laplacian spectra in $(\log s, L(s))$-coordinates. Upper panel – continuous zone of spectrum, lower panel – discrete zone of spectrum: (a–b) Data from Hagmann et al. [21]; (c–d) Data from Open Connectome Project [25]; (e–f) Barabasi-Albert network. Slope = 1 (blue dashed curve) indicates the Poissonian statistics, slope = 2 (red dashed curve) indicates the Wigner-Dyson regime.

where $C(s)$ is the cumulative distribution of s. The main question is whether the level spacing distribution of human connectomes obeys the Wigner surmise, i.e. demonstrates the level repulsion typical for interacting chaotic systems, shares the Poisson statistics, which means that the eigenvalues are uncorrelated, or enjoys criticality? The results of our computations for Laplacian matrices of human connectomes are presented in Fig. 3.

The computational algorithm is as follows. As one can see from Fig. 2, the spectral density of adjacency matrix, A, of a human connectome consists of a continuous (central) zone and a set of separated peaks (discrete zone, one separated eigenvalue per one cluster). In the Laplacian L, defined in (1), one can also split the spectral density into continuous and discrete parts. In each such part we determine the intervals Δ, within which the level spacing belongs either to delocalized (Wigner-Dyson), or to localized (Poissonian) subparts. Two regimes in $P(s)$ (both in continuous and discrete part of the spectrum) are connected by the crossover region which corresponds to the transition from Wigner to Poissonian statistics. The level spacing of two human connectomes are shown in Fig. 3(a, c) for the continuous part of the spectrum, and in Fig. 3(b, d) for the discrete one. In Fig. 3(e) we have plotted for comparison the level spacing of Barabasi-Albert network Laplacian in the discrete part of the spectrum. No crossover is seen and all eigenvalues are localized. We have analyzed the human connectomes only due to lack of statistics for other organisms.

The level spacings of the Laplacian matrices of two analyzed human connectomes demonstrate "hybrid" behavior with a clear-cut crossover from Wigner-Dyson to Poisson statistics in each part of the spectrum as a function of s. Such a behavior matches the universal form of $P(s)$ discovered in the 3D Anderson localization for systems at criticality – see [42]. The conjecture about the human connectome criticality is a highly debated issue (see [43,44] for contemporary discussions). Certainly, the criticality conjecture is very attractive since in this regime one has naturally the long-wave excitations and effective collective processing of the information. Our result provides a strong support for the criticality of the structural human connectome from the standard spectral analysis viewpoint widely used in condensed matter physics.

3. Discussion

3.1. Main conclusions

The experimental analysis of brain networks is rather complicated issue due to the lack of available experimental data. The human brain is made up of 8.6×10^{10} neurons [23], and current imaging techniques do not allow resolving

complete microscopic connectivity. Only neuronal connectomes of comparatively primitive organisms, such as C. intestinalis and a C. elegans nematode, are yet available. The nematode connectome reconstruction had started in 1974 and lasted 12 years, despite it contains only about 300 neurons and several thousands of synaptic connections [24]. In a huge number of works the brain networks are studied at large and middle scales. That introduces additional difficulties in the process of comparing brain networks of different organisms.

The idea of randomizing a network with preserving degrees of nodes (the Maslov-Sneppen algorithm) is not new, however in the literature it has been used typically out of the context of the spectral graph theory, being applied mainly to the determination of the average path length in the network, the global clustering coefficient, etc. In our work, following the ideas developed in [27], we use the Maslov-Sneppen randomization in combination with the spectral analysis. This allows us to uncover some hidden structural properties of network samples and analyze the stability of the spectrum with respect to the network topological rearrangement. We have proposed the procedure to identify differences in the architecture of the connectomes of the organisms which stay on different steps of the evolutionary staircase.

The results of our study clearly demonstrate that some fundamental properties of the connectome cannot be explained by the behavior of typical network characteristics, such as the vertex degree distribution, the averaging clustering coefficient and the distribution of clustering among network nodes. This is especially true for human connectomes, for which we have shown that the "earth mover's distance" (EMD) between the structural network pattern (represented by the adjacency matrix) and its randomized "null state" network, is essentially larger than respective EMDs for other animals. Such an interpretation raises a natural question about the significance of differences in the spectra of macaque and human connectomes, which evolutionary are much closer to each other than the human to the nematode. As one sees from Table 1, the connectomes of macaque and human are both poorly restored by the "first level" TPC algorithm, while reasonably well – by the "second level" LCC one. To the contrary, the connectomes of C. elegans and C. intestinalis are reconstructed sufficiently well already by the first-level TPC algorithm.

We have performed crosscheck of our results on various sets of data to avoid the artifacts of specific algorithms of neurobiological data available from open sources. For this purpose we have used different human connectome data sets obtained by various experimental methods. Also, the sizes of considered networks varied from several hundred to several thousand nodes. However, for macaque such precautions are not yet possible, since the CoCoMac project data [8] is the only one complete source of information for the brain connectivity of macaque connectome.

The distribution of triangles for each vertex of the network seems to be a simplest invariant preserving the shape of the network spectrum. Keeping only the average clustering coefficient (TPC), we are unable to restore the spectrum of the network from its randomized version. For better reconstruction of the network topology it is not sufficient to know how many triangular motifs the network has in average (TPC), but it is crucial how these triangles are distributed among the nodes (LCC). The vectors of triangular motifs, $\mathbf{T}$, in the real network pattern and in its randomized versions are not identical. Apparently, knowing $\mathbf{T}$ is crucial for reconstruction a modular brain architecture with several coupled hierarchical levels. The importance of local clustering has been repeatedly highlighted in the analysis of brain networks [19,45]. It is suggested that the combination of the high local connectivity and the "small world" property on large scales is responsible for many features of a brain functioning [46]. Perhaps, the local clustering should be considered as a crucial achievement of evolutionary selection, which essentially distinguishes the connectome from its randomized version.

We have provided an analysis of the eigenvalue correlations in spectra of Laplacian matrices of structural connectomes. We found that the level statistics is critical. This finding supports the widely discussed controversial issue of the brain criticality, formulated long time ago [47]. There are many arguments in favor and against this hypothesis and our spectral analysis yields one additional support of criticality based on a pure statistical analysis.

In our study we worked with the undirected structural networks which certainly restricts the reliability of our findings. However, even for non-oriented structural connectome the spectral analysis provides the new important insights. Recent studies [48] of oriented structural connectome show that new interesting features emerge which definitely deserve elaborations of a new reliable mathematical models and clear physical explanations.

The issue of uniqueness of the human brain in its cognitive abilities and conscious information processing has been widely addressed at various levels of analysis, including evolutionary expansion of selective regions of the cerebral cortex, emergence of specific properties in the human neocortical neurons, novel kinds of cellular interactions, new molecular pathways, specificity of gene expression in neuronal and glial cortical cells [49–54]. Our work contributes to another dimension of this analysis by pointing at the peculiarity of the human connectome global organization. The

spectral characteristics of human connectome support an expanded range of criticality known to maximize information transmission, sensitivity to external stimuli and coordinated global behavior typical of conscious states [55–59].

3.2. Directions for further research

The challenging question deals with understanding interaction and synchronization of various functional sub-networks in the connectome. The first step on this way consists in the consideration of a two-layer network where there is a competition between strength of open in-layer 3-motifs and cross-layer pairwise interactions. In [60] it has been found that within such a model one can see the phase transition between the phases with dominance of in-layer– or cross-layer–connections. Depending on the parameters of the model, these two phases can be separated either by the sharp boundary, or can be transformed one into another smoothly. One can think about the applicability of a two-layer network for the description of functional interactions between the hemispheres. As pointed in [36], the presence of open 3-motifs in each hemisphere is crucial for the effective informational flow inside the hemisphere, while the links between hemispheres are evidently important for the entire brain functioning. The existence of the phase transition in the abstract two-layer dynamic network considered in [60], allows one to suggest that in functional brain networks the competition between in-layer and cross-layer interactions occurs either as a sharp 1st order phase transition which might be associated with the brain disease, or as a smooth crossover.

A bunch of questions concerns the observed criticality of the connectome, many of them have been already posed in the literature. The most immediate question deals with the role of the long-wave excitations intrinsic for the critical regime in the brain functioning. To make the problem more tractable, one can apply the full machinery of the critical regime analysis borrowed from the condensed matter physics. For example, the fractal dimension and the spectral dimension can be evaluated. Most of the results concerning the criticality deal with the avalanches in the neuron spiking phenomena (incomplete list of the references includes [61–70]). Our results imply that the structural connectome organization supports the critical behavior of neural excitations.

The abstract two-layer network evolving via Maslov-Sneppen rewiring algorithm, with in-layer and cross-layer interactions, demonstrate also a kind of synchronization behavior. Increasing the energy of in-layer motifs *in one layer only*, we can force the clustering in *both* layers simultaneously. Such a synchronization is the consequence of joint conservation laws in the full rewired network. It is worth noting that the multi-layer networks can demonstrate a bunch of new critical phenomena [71,72], such as collective phase transitions (see [73] for the review) which are absent in single-layer networks.

Understanding the interplay between the spectral properties of the structural connectome and the informational capacity of the brain is crucial for the consciousness problem [74]. The discussions on this topic deals with the concept of the "integrated information" proposed in [75]. Though its initial formulations were of very limited practical applicability, the last refinements of this theory [76] use the standard tools of the spectral analysis of random networks, which makes the evaluation of the integrated information more tractable. Besides, it seems highly desirable to interpret the aspects of consciousness using the standard notions of statistical and quantum physics, such as the entanglement entropy, entanglement negativity and complexity – see [77] for the review. It is highly likely that the free energy extremization discussed in [78] could be of use for the description of the brain organization.

Since the clustered networks allow the natural embedding into the hyperbolic geometry [79], it might be possible to use modern holographic approach for the evaluation of the entanglement entropy [80] and the complexity [81, 82] via the geometry of the hyperbolic space. Some of these ideas have been already implemented in [83,84] in terms of random networks of special architecture. We believe that the progress in the field of brain studies lies at the edge of spectral theory, statistical mechanics of complex entangled systems and holography. Some initial discussion concerning the possible interplay between the criticality of the connectome and the holographic approach can be found in [85].

4. Methods

4.1. Randomization algorithms and spectral density of constrained Erdős-Rényi network

The evolution of the network is carried out using the Metropolis algorithm, which can be described as follows: taking the "null network state" as the input, the algorithm attempts to make random rewiring in the network. If these

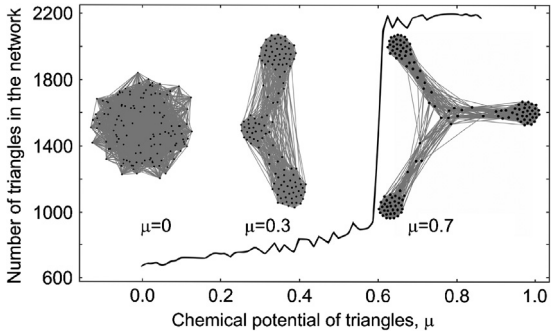

Fig. 4. Phase diagram of for constrained Erdős-Rényi networks. Number of triangles in the final network has a jump at the point $\mu = \mu_{crit}$ which for large networks corresponds to 1st order phase transition. Typical network structures are shown at three different values of μ.

changes occur in a "right direction", i.e. reduce the distance between the current and the desired state of the network in a pre-selected metric, they are accepted with probability one. If, to the contrary, the elementary rewiring pushes the network away from the desired state (for example, reduces the number of triangular motives, though the purpose of the evolution is to increase them), it is accepted with some probability, exponentially decreasing with the size of "wrong" deviation. The chemical potential, μ, is a parameter, governing the probability of the "wrong" step in the network evolution. The chemical potential approves its name by the function it performs: bringing analogy from physics, μ controls the amplitude of "thermal fluctuations" in the algorithm known as "simulated annealing": in the absence of thermal fluctuations, the network accepts only "positive changes" in its evolution along the landscape and might be easily trapped in a local energy minima. The possibility of "backward moves" allows the system to escape from local traps, thus helping the network to reach the true ground state.

One can easily understand the sense of an evolutionary algorithm on example of rewiring of the constrained Erdős-Rényi network (CERN) of N nodes. CERN evolves under the condition that the vertex degree in each node is conserved. The spectral properties of CERNs were thoroughly investigated in [27]. The "driving force" of the network's evolution is the attempt to increase the number of closed 3-motifs (closed triad of links).

The condition of the vertex degree conservation in each node changes drastically the final state of the evolving structural network. The constraints provide N conservation laws for the stochastic rewiring making the corresponding dynamic system quite special. In particular, it was found in [27] that the evolving CERN undergoes the phase transition and gets defragmented into a set of K dense communities when the chemical potential, μ, of closed 3-motifs exceeds some critical value, μ_{cr}. The number of communities, K, depends on the density of the network at the preparation conditions and can be approximately estimated as $[1/p]$, where $[...]$ designates the integer part of $1/p$ and p is a probability to connect any two randomly chosen vertices of the Erdős-Rényi network. The phase diagram of the random CERN enriched by closed 3-motifs (controlled by the chemical potential μ) is shown in Fig. 4. To make the figure more informative, we show network samples at three different densities of closed 3-motifs. The effective way of constructing the phase diagram is discussed below.

We have mentioned already that in constrained Erdős-Rényi networks with stochastic rewiring, the clustering occurs when the evolving network tends to increase the number of closed 3-motifs (triangles), $n_{\triangle}$. The concentration of triangles is fixed by the chemical potential, μ. Imposing the condition of the vertex degree conservation in course of network rewiring, together with the condition of maximization the number of closed 3-motifs, one forces the network to clusterize respecting the conservation laws. The detailed analysis of phase transitions in CERN has been carried out in [27] where it was found that the condition of maximization of number of closed triads forces the random network with the conserved vertex degree to form a multi-clique ground state (see Fig. 4). At $\mu = \mu_c$ the network experiences the first order phase transition and splits in the collection of weakly connected clusters.

The structure of clusters (cliques) was carefully studied in [27] via the spectral analysis of the matrix A of the network. It has been shown that at $\mu < \mu_c$, the spectral density has the shape typical for Erdos-Renyi graphs with moderate connection probability, $p = O(1) < 1$, being the Wigner semicircle with a single isolated eigenvalue apart. At μ_c the eigenvalues decouple from the main core and a collection of isolated eigenvalues forms the second (non-perturbative) zone as it is shown in Fig. 5a. The number of isolated eigenvalues coincides with the number of clusters formed above μ_c. Averaging over ensemble of graphs patterns smears the distribution of isolated eigenvalues in the

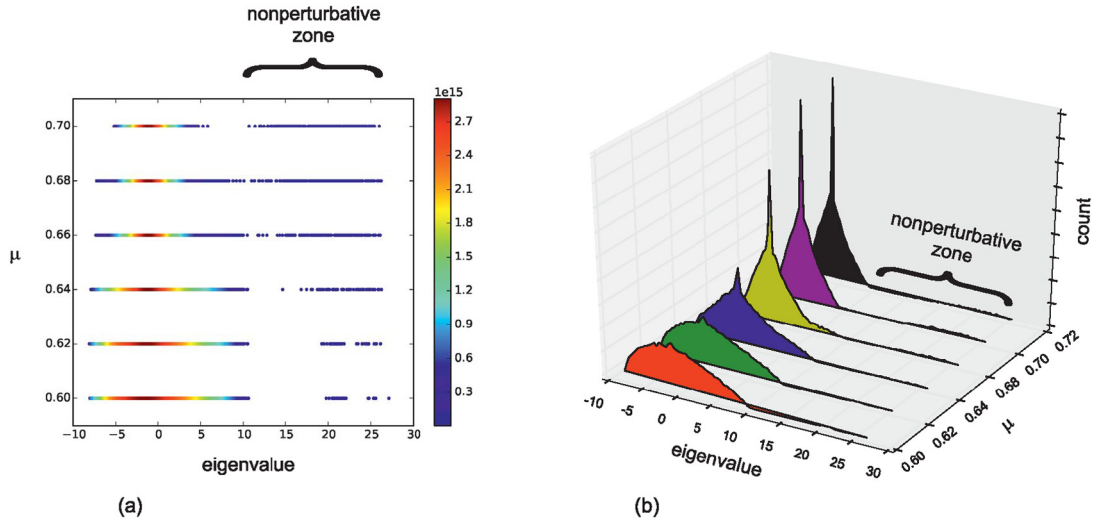

Fig. 5. (a) The spectral density of ensemble of constrained Erdős-Rényi graphs for various chemical potentials μ of closed 3-motifs; (b) The same as (a) in a three-dimensional representation. The numerical results are obtained for the ensembles of 50 Erdős-Rényi graphs of 256 vertices and the bond formation probability $p = 0.08$.

second zone. Above μ_c the support of the spectral density in the first (central) zone shrinks and the second zone becomes dense and connected. The modes in the second zone are all localized, while the ones in the central zone remain delocalized. The evolution of the spectral density of the entire network is depicted in Fig. 5b. The numerical results on spectral density evolution are obtained for the ensembles of 50 Erdős-Rényi graphs of 256 vertices each and the bond formation probability $p = 0.08$.

Two important properties of the spectral density of adjacency matrices of constrained Erdős-Rényi networks have to be mentioned:

- The spectral densities of each cluster (clique) and of the whole network are very different [27]. The spectrum of a clique is discrete, while the spectrum of the whole network has a two-zonal structure with the continuous triangle-shape form of the first (central) zone. We have interpreted this effect as the collectivization (or synchronization) between the modes in different clusters.
- There is a memory of the spectrum in the central zone on the initial state (on the preparation conditions), which is the signature of the non-ergodic nature of the system and of the presence of some hidden conservation laws [86].

4.2. Motif-driven network evolution

The numerical procedure which manipulates by the experimental data on structural connectomes taken from open sources is described below. We are aimed to reveal the principle "conservation laws" which govern the structural transformation of the connectome during the biological evolution.

There is a common belief supported by many numerical simulations that the spectral density of a graph adjacency matrix is a "fingerprint" of a corresponding network in generic situation. Besides, there are known examples of "isospectral" graphs which have different adjacency matrices, however their spectra coincide. Such situations are rather exceptional and practically do not occur in randomly generated patterns (their Kolmogorov complexity is very high). In our study we consider the spectral density as a graph invariant which sets a "metric" for graphs: if spectral densities of two graphs are similar, we say that the adjacency matrices are similar; as less two spectral densities resemble each other, as more unlike are the graphs. For the quantitative comparison of spectral densities we use the "transport" (or "earth mover's") metric – see [37] for precise definition. Thus, rewiring the network, we catch the evolution of the corresponding spectral density.

Setting of numerical simulations is as follows. We take structural connectomes (the state S) of C. elegans, C. intestinalis, macaque and human, defined by adjacency matrices of corresponding networks, and destroy the network

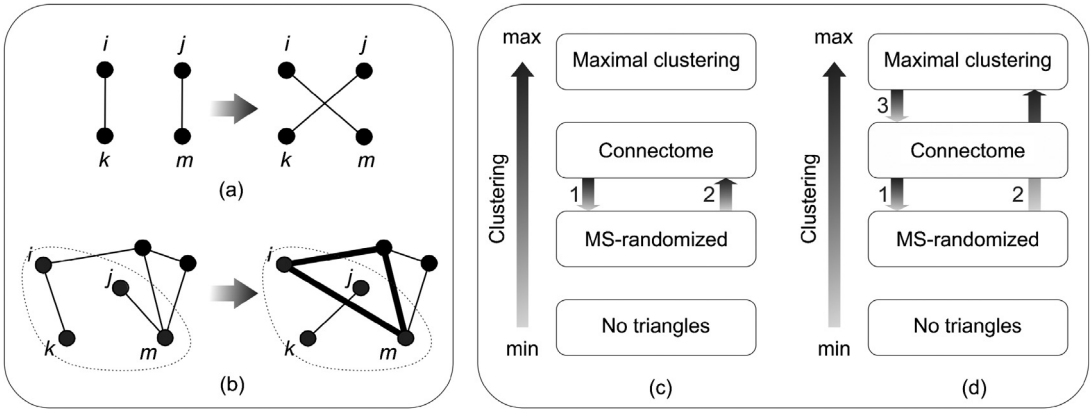

Fig. 6. (a) Single rewiring step of a Maslov-Sneppen algorithm preserving degrees of all vertices; (b) Example of a local network updating which increases the number of triangles; (c)-(d) Schematic realization of evolutional algorithm described in the paper: (c) structural connectome network is randomized via Maslov-Sneppen algorithm (arrow 1) and then restored again under the control of the average number of triangles or the clustering coefficient (arrow 2), (d) practical implementation of algorithm consists of randomizing network (arrow 1), transferring network to maximally clustered state (arrow 2) and then restoring the connectome under the control of the average number of triangles or the clustering coefficient (arrow 3).

patterns by random rewiring of links under the condition of the vertex degree conservation at each graph node, thus getting the state S_{rand} (the "null state"). To obtain the null-state networks, we used the Maslov-Sneppen randomization (MS) algorithm [38] – see Fig. 6(a-b). The rewiring procedure retains the size of the network and its density, and also strictly preserves the degree of all nodes. Degree distribution was shown to be of key importance for the network's structure, that is why we consider MS-randomized networks as "null-state" patterns. Despite the vertex degree distribution of randomized (S_{rand})- and initial (S)-networks is the same, their topological, motif, spectral and other properties can be essentially different.

Now, starting from the state S_{rand}, we are trying to recover back the S-state by the random rewiring of links (again with the vertex degree conservation), however now – under the influence of a "driving force" via the Metropolis algorithm towards a state with a given density of closed 3-motifs. The closeness of two network states, the initial and the one, restored from the randomized one, is measured by the earth mover's distance between their spectra.

The standard Maslov-Sneppen Metropolis algorithm described above is transparent and straightforward in implementation. However, performing evolution of MS-randomized network to a highly clustered state, requires a lot of computational resources: it takes much more time to pull the network evolution towards a state with a given density of closed 3-motifs, than to push it to the "null state". To reduce the computational time, we have implemented another procedure which leads to the same result. Instead of starting from a completely randomized network state with a preserved degree distribution, we constructed a *maximally clustered* network (MCN) (again respecting the vertex degree conservation). The MCN is a graph that has maximal (or nearly maximal) number of closed 3-motives available for a given degree distribution.

Taking maximally clustered network as a "null state" and running the Maslov-Sneppen Metropolis procedure controlled by the density of closed 3-motifs, we bring the network to desired clustering level. Such a technical trick allows to perform computations for highly clustered graphs very efficiently. Figuratively, one can say that assembling the network with specified density of closed 3-motifs from the randomized state is like a "rising to the mountain", while reconstructing the network from maximally clustered state is like a "descending from the mountain", which is less energy consuming. Schematically we have depicted these two algorithms in Fig. 6(c-d).

So, we have two types of "null-state" networks: the MS-randomized network and MCN. Selection between them depends on the choice between the clustering evolution in "up" or "down" directions. In our work we use two types of additional constraints imposed on the null-state network evolution:

- The "first level" triangle-preserving constraint (TPC) is the condition of maximizing the number of closed 3-motifs in the evolving graph until its clustering reaches the level of the initial (pattern) network. Using this procedure, we calculate the total number of triangles in the network, while we do not pay attention how these

triangles are distributed over the network nodes. In general, such an "averaged clustering preserving procedure" allows to get a network state which is closer to the original one than the simple MS-randomized network.

- The "second level" local clustering constraint (LCC) preserves local clustering in each node of the network. The rewired network preserves (besides to vertex degree conservation) the number of closed 3-motifs in each node. The implementation of the LCC algorithm is thoroughly described below.

4.3. Network randomization with additional conservation laws

More refined algorithms of network's rewiring are requested to conserve simultaneously several characteristics of the original graph. We are guided by an attempt to propose the "minimal" model which, on one hand, could capture the key properties of the structural connectome and could distinguish humans from other organisms, and on the other hand, is as simple as possible. We put forward the conjecture that such additional feature that should be conserved during the network randomization together with the vertex degree conservation, is the number of triangles in which each node participates.

We randomize the network, conserving in all nodes: i) the vertex degree; ii) the clustering coefficient. We propose our own way to solve this problem numerically using the modification of the Metropolis algorithm. Having the network adjacency matrix, $A = \{a_{ij}\}$, of a graph $((i, j) = 1, \ldots, N)$, consider two auxiliary diagonal matrices, $D_\star$, $D_\triangle$, defined as follows

$$\begin{cases} D_\star = \{d_1, d_2, \ldots, d_N\}: & d_i = \sum_{j=1}^{N} a_{ij} \\ D_\triangle = \{\tilde{d}_1, \tilde{d}_2, \ldots, \tilde{d}_N\}: & \tilde{d}_i = \sum_{j\neq k}^{N} a_{ij} a_{jk} a_{ki} \end{cases} \tag{4}$$

The elements of the matrix $D_\star$ are the degrees of nodes, while the elements of the matrix $D_\triangle$ are the numbers of triangles into which a specific node is involved. Our algorithm resembles the simulation of some physical process that occurs when a substance crystallizes. It is assumed that the "crystal lattice" has already been formed, however the transitions of "individual atoms" from site to site are still permissible.

It is assumed that the destination state of the network is the configuration in which clustering of all nodes is the same as in the "pattern state" (there are many such destination networks). Our algorithm takes the "null state" randomized network in which the information about the clusterization in the initial pattern is "washed out". Then we rewire the network, conserving all the degrees of nodes. After each rewiring, we compute the discrepancy F between the resulting modified network and the preselected pattern network

$$F = \sum_{i=1}^{N} |C_i - C_{i0}| \tag{5}$$

where N is the number of nodes, C_i is the clustering coefficient of the node i in the evolving network, while C_{i0} is the clustering coefficient in the pattern network which the evolving network tends to reach. Another definition of the discrepancy which sets the metric in the space of the "networks similarity", T, is as follows

$$T = \sum_{i=1}^{N} |T_i - T_{i0}| \tag{6}$$

This definition is equivalent to (5), except that the clustering coefficient is replaced by T_i, where T_i is the absolute number of triangles involving the vertex i.

The Metropolis-like algorithm which minimizes both cost functions, F and T, is set as follows. First, we chose the metrics (5) or (6). If the local random perturbation (rewiring) of the network is such that the system tends to the desired destination state (i.e. F or T decrease), this random step is accepted with the probability 1. Otherwise, if F or T are increased by $\Delta \geq 0$ in the selected metric, the corresponding step is accepted with the probability $e^{-\mu\Delta}$, where $\mu > 0$ is the chemical potential of Metropolis procedure. After reaching the local energy minimum (which is calculated on the basis of the best time/distance ratio), the algorithm updates the metric and repeats the procedure. Such an algorithm known as the "simulated annealing", allows to reach the ground state of the system without getting trapped at local minima in the very complex energy landscape.

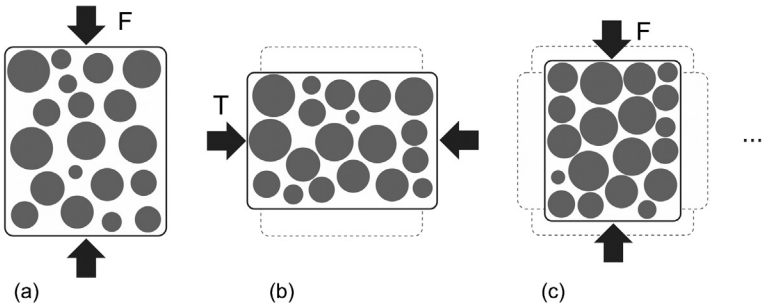

Fig. 7. Illustration of a repetitive sequential minimization of F and T. Minimizing F we compress the pile, however can slightly increase T. Minimizing T afterwords, we compress the pile further, however could slightly increase F. Repeating $F - T - F - \ldots$ compression and shacking randomly the pile, we reach the densest packing.

Computing the discrepancy between the evolving network ad its final destination via the clustering coefficients, F, we "equalize" nodes with different vertex degrees. Namely, for all nodes the clustering coefficient lies between 0 and 1. Thus, nodes with low degrees, "pull" the triangles from hubs during the network evolution as they are widely spread. On the other hand, the rewiring procedure via T-metric satisfies the interests of large nodes to the detriment of small ones. We have developed the optimization procedure in which both metrics F and T are simultaneously used. The algorithm sequentially switches between these metrics and adjusts the network for both F, respecting the interests of loosely connected nodes, and T, which works well for hubs. Schematically the implementation of the algorithm is depicted in Fig. 7 on the example of sphere packing. Vertical compression (associated with the minimization of F) of the random 2D pile of spheres leads to a desired increase of the density, however might be accompanied by the increase of a horizontal size (associated with T). To squeeze the pile more, we shake the pile randomly and compress it in the horizontal direction, then we switch back to the vertical compression, etc., until the densest packing state is reached.

Arriving at the stationary state, when F and T cannot be decreased anymore during reasonable time, we compare the adjacency matrices of the destination network with the preselected pattern by comparing the corresponding spectra of two matrices. The distance between spectra (which, by virtue of the above comments about the uniqueness of the spectrum, is understood as a quantitatively expressed degree of the "dissimilarity" of the two networks) is measured in terms of the "earth mover's distance" metric (or Wasserstein's metric).

4.4. Spectral distance

All plotted network spectra were constructed by simple convolution of the set of eigenvalues with a Gaussian distribution and further normalization to make the area under the curve equal to 1. To have the quantitative characteristics of the difference between spectral densities, we have computed the earth mover's distance (EMD), E, between spectral densities.

The EMD is a metric based on the minimum cost of transforming one histogram into another. Representing two distributions (two spectral densities) as two heaps of earth that need to be superposed by transferring small pieces of earth, EMD determines the least amount of work required to accomplish this task. The calculation of EMD is based on solving the transport linear programming problem, for which effective algorithms are known. In our work we were using an open-source Python package designed for fast EMD computation [39,37].

4.5. Data availability

Data on the macaque connectome is limited to the only one network obtained in the Cocomac project [8]. Data on C. elegans and macaque connectomes have been taken from the Open Connectome Project [25] database. Data on human structural connectomes were extracted both from Open Connectome Project and Human connectome project databases [26]. We have also performed our analysis for brain network of a cat [7] containing 64 nodes, however, it was too small to obtain statistically significant results and thus was excluded from the final comparison. All the software required for network analysis performed was created on Python and are available at our github repository.

Author contributions

A.G., S.N. and N.P. designed the experiments. N.P. and O.V. performed the numerical simulations. V.A., K.A., A.G., S.N. and N.P. analyzed the results. All authors contributed and reviewed the manuscript.

Competing interests

The authors declare that they have no competing interests.

Acknowledgements

We are grateful to A. Kamenev for the important comments. The work of V.A. was supported within frameworks of the state task for ICP RAS 0082-2014-0001 (state registration AAAA-A17-117040610310-6). S.N. is grateful to RFBR grant 18-23-13013 for the support. The work of A.G. was partially supported by the Basis Foundation Fellowship and RFBR grant 19-02-00214. N.P. and O.V. acknowledge the support of the RFBR grant 18-29-03167. O.V. thanks Basis Foundation Fellowship for the support. A.G. thanks SCGP at Stony Brook University and KITP at University of California, Santa Barbara, for the hospitality.

References

[1] Sporns O. Networks of the brain. Cambridge, MA: MIT Press; 2011.
[2] Sporns O. Discovering the human connectome. Cambridge, MA: MIT Press; 2012.
[3] Fornito A, Zalesky A, Bullmore E. Fundamentals of brain network analysis. Amsterdam: Elsevier. ISBN 978-0-12-407908-3, 2016.
[4] Kaiser M. A tutorial in connectome analysis: topological and spatial features of brain networks. NeuroImage 2011;57:892.
[5] Varshney LR, Chen BL, Paniagua E, Hall DH, Chklovskii DB. Structural properties of the Caenorhabditis elegans neuronal network. PLoS Comput Biol 2011;7:e1001066.
[6] Gastner MT, Õdor G. The topology of large Open Connectome networks for the human brain. Sci Rep 2016;6:27249.
[7] Scannell JW, Blakemore C, Young MP. Analysis of connectivity in the cat cerebral cortex. J Neurosci 1995;15:1463.
[8] Stephan KE, Kamper L, Bozkurt A, Burns GA, Young MP, Kötter R. Advanced database methodology for the collation of connectivity data on the macaque brain (CoCoMac). Philos Trans R Soc Lond B, Biol Sci 2001;356:1159.
[9] van den Heuvel MP, Scholtens LH, de Reus MA. Topological organization of connectivity strength in the rat connectome. Brain Struct Funct 2015;221:1719.
[10] Watts DJ, Strogatz SH. Collective dynamics of small-world networks. Nature 1998;393:440.
[11] Dorogovtsev SN, Goltsev AV, Mendes JFF. Critical phenomena in complex networks. Rev Mod Phys 2008;80:1275.
[12] Nadakuditi RR, Newman MEJ. Graph spectra and the detectability of community structure in networks. Phys Rev Lett 2012;108:188701.
[13] Nadakuditi RR, Newman MEJ. Spectra of random graphs with arbitrary expected degrees. Phys Rev E 2013;87:012803.
[14] Eguiluz VM, Chialvo DR, Cecchi GA, Baliki M, Apkarian AV. Scale-free brain functional networks. Phys Rev Lett 2005;94:018102.
[15] Barabasi AL, Albert R. Emergence of scaling in random networks. Science 1999;286:509.
[16] Latora V, Marchiori M. Efficient behavior of small-world networks. Phys Rev Lett 2001;87:198701.
[17] Mathias N, Gopal V. Small worlds: how and why. Phys Rev E, Stat Nonlinear Soft Matter Phys 2001;63:021117.
[18] Sporns O. Small-world connectivity, motif composition, and complexity of fractal neuronal connections. Biosystems 2006;85(55).
[19] Kim JS, Kaiser M. From Caenorhabditis elegans to the human connectome: a specific modular organization increases metabolic, functional and developmental efficiency. Philos Trans R Soc Lond B, Biol Sci 2014;369:1653.
[20] de Lange SC, van den Heuvel MP, de Reus MA. The Laplacian spectrum of neural networks. Front Comput Neurosci 2014;7:189.
[21] Hagmann P, Cammoun L, Gigandet X, Meuli R, Honey CJ, Wedeen VJ, et al. Mapping the structural core of human cerebral cortex. PLoS Biol 2008;6:E159.
[22] Yamaguti Y, Tsuda I. Mathematical modeling for evolution of heterogeneous modules in the brain. Neural Netw 2015;62(3).
[23] Azevedo FA, Carvalho LR, Grinberg LT, Farfel JM, Ferretti RE, Leite RE, et al. Equal numbers of neuronal and nonneuronal cells make the human brain an isometrically scaled-up primate brain. J Comp Neurol 2009;513:532.
[24] White GG, Southgate E, Thomson JN, Brenner S. The structure of the nervous system of the nematode Caenorhabditis elegans. Philos Trans R Soc Lond B, Biol Sci 1986;314(1).
[25] Kiar G, et al. neurodata/ndmg: stable ndmg-DWI pipeline release. Zenodo; 2018.
[26] Brown JA, Rudie JD, Bandrowski A, Van Horn JD, Bookheimer SY. The UCLA multimodal connectivity database: a web-based platform for connectivity matrix sharing and complex network analysis. Front Neuroinform 2012.
[27] Avetisov V, Hovhannisyan M, Gorsky A, Nechaev S, Tamm M, Valba O. Eigenvalue tunneling and decay of quenched random networks. Phys Rev E 2016;94:062313.
[28] Colomer-de-Simón P, Serrano M, Beiró MG, Alvarez-Hamelin J, Boguñá M. Deciphering the global organization of clustering in real complex networks. Sci Rep 2013;3:2517.

[29] Sporns O, Honey CJ, Kötter R. Identification and classification of hubs in brain networks. PLoS ONE 2007;2:E1049.
[30] Harriger L, van den Heuvel MP, Sporns O. Rich club organization of macaque cerebral cortex and its role in network communication. PLoS ONE 2012;7:E46497.
[31] Meunier D, Lambiotte R, Bullmore ET. Modular and hierarchically modular organization of brain networks. Front Neurosci 2010;4:200; Basett DS, Bullmore ET. Small-world brain networks. Neuroscientist 2006;12:512.
[32] Taylor P, Wang Y, Kaiser M. Within brain area tractography suggests local modularity using high resolution connectomics. Sci Rep 2017;7:39859.
[33] Gollo LL, Mirasso C, Sporns O, Breakspear M. Mechanisms of zero-lag synchronization in cortical motifs. PLoS Comput Biol 2014;10:e1003548.
[34] Gollo LL, Zalesky A, Hutchison RM, van den Heuvel M, Breakspear M. Dwelling quietly in the rich club: brain network determinants of slow cortical fluctuations. Philos Trans R Soc Lond B, Biol Sci 2015;370:20140165.
[35] Moretti P, Munoz MA. Griffiths phases and the stretching of criticality in brain networks. Nat Commun 2013;4.
[36] Wang MB, Owen JP, Mukherjee P, Rai A. Brain network eigenmodes provide a robust and compact representation of the structural connectome in health and disease. PLoS Comput Biol 2017;22:E1005550.
[37] Pele O, Werman M. Fast and robust earth mover's distances. In: Proc. 2009 IEEE 12th int. conf. on computer vision; 2009. p. 460–7.
[38] Maslov S, Sneppen K. Specificity and stability in topology of protein networks. Science 2002;296:910.
[39] Pele O, Werman M. A linear time histogram metric for improved SIFT matching. In: Computer vision - ECCV; 2008. p. 495–508.
[40] Gomez S, Diaz-Guilera A, Gomez-Gardeñes J, Perez-Vicente CJ, Moreno Y, Arenas A. Diffusion dynamics on multiplex networks. Phys Rev Lett 2013;110:028701.
[41] Mehta ML. Random matrices. Academic Press; 1991.
[42] Shklovskii BI, Shapiro B, Sears BR, Lambrianides P, Shore HB. Statistics of spectra of disordered systems near the metal-insulator transition. Phys Rev B 1993;47:11487.
[43] Beggs JM, Timme N. Being critical of criticality in the brain. Front Physiol 2012.
[44] Cocchi L, Gollo LL, Zalesky A, Breakspear M. Criticality in the brain: a synthesis of neurobiology, models and cognition. Prog Neurobiol 2017.
[45] Sohn Y, Choi MK, Ahn YY, Lee J, Jeong J. Topological cluster analysis reveals the systemic organization of the Caenorhabditis elegans connectome. PLoS Comput Biol 2011;7:E1001139.
[46] Sporns O. The human connectome: a complex network. Ann NY Acad Sci 2011;1224:109.
[47] Freeman WJ. Simulation of Chaotic EBG patterns with a dynamic model of the olfactory system. Biol Cybern 1987;56:139.
[48] Reimann M, Nolte M, Scolamiero M, Turmer K, Perin R, Chindemi G, et al. Cliques of neurons bound into cavities provide a missing link between structure and function. Front Comput Neurosci 2017;11(48).
[49] Smaers JB, Gómez-Robles A, Parks AN, Sherwood CC. Exceptional evolutionary expansion of prefrontal cortex in great apes and humans. Curr Biol 2017;714.
[50] Florio M, Borrell V, Huttner WB. Human-specific genomic signatures of neocortical expansion. Curr Opin Neurobiol 2017;42(33).
[51] He Z, Han D, Efimova O, Guijarro P, Yu Q, Oleksiak A, et al. Comprehensive transcriptome analysis of neocortical layers in humans, chimpanzees and macaques. Nat Neurosci 2017;20:886.
[52] Somel M, Liu X, Khaitovich P. Human brain evolution: transcripts, metabolites and their regulators. Nat Rev Neurosci 2013;14:112.
[53] Sousa AMM, Zhu Y, Raghanti MA, Kitchen RR, et al. Molecular and cellular reorganization of neural circuits in the human lineage. Science 2017;358:1027.
[54] Hardingham GE, Pruunsild P, Greenberg ME, Bading H. Lineage divergence of activity-driven transcription and evolution of cognitive ability. Nat Rev Neurosci 2018;19(9).
[55] Vázquez-Rodríguez B, et al. Stochastic resonance at criticality in a network model of the human cortex. Sci Rep 2017;7:13020.
[56] Kinouchi O, Copelli M. Optimal dynamical range of excitable networks at criticality. Nat Phys 2006;2:348.
[57] Haldeman C, Beggs J. Critical branching captures activity in living neural networks and maximizes the number of metastable states. Phys Rev Lett 2005;94:058101.
[58] Shew WL, Yang H, Petermann T, Roy R, Plenz D. Neuronal avalanches imply maximum dynamic range in cortical networks at criticality. J Neurosci 2009;29:15595.
[59] Tagliazucchi E. The signatures of conscious access and its phenomenology are consistent with large-scale brain communication at criticality. Conscious Cogn 2017;55:136.
[60] Avetisov V, Gorsky A, Maslov S, Nechaev S, Valba O. Phase transitions in social networks inspired by the Schelling model. Phys Rev E 2018;002300.
[61] Brochini L, Costa AA, Abadi M, Roque AC, Stolfi J, Kinouchi O. Phase transitions and self-organized criticality in networks of stochastic spiking neurons. arXiv:1606.06391.
[62] Chialvo DR. Emergent complex neural dynamics. Nat Phys 2010;6:744.
[63] Hesse J, Gross T. Self-organized criticality as a fundamental property of neural systems. Front Syst Neurosci 2014;8.
[64] Lombardi F, Herrmann H, Perrone-Capano C, Plenz D, De Arcangelis L. Balance between excitation and inhibition controls the temporal organization of neuronal avalanches. Phys Rev Lett 2012;108:228703.
[65] Beggs JM. The criticality hypothesis: how local cortical networks might optimize information processing. Philos Trans R Soc Lond A, Math Phys Eng Sci 2008;366:329.
[66] Shew WL, Yang H, Petermann T, Roy R, Plenz D. Neuronal avalanches imply maximum dynamic range in cortical networks at criticality. J Neurosci 2009;29:15595.
[67] De Arcangelis L, Lombardi F, Herrmann H. Criticality in the brain. J Stat Phys Theory Exp 2014:P03026.

[68] Schuster H. Criticality in neural systems. John Wiley & Sons; 2014.
[69] Tgliazucchi E. The signatures of conscious access in phenomenology is consistent with large-scale brain communication at criticality. Conscious Cogn 2017;55:136.
[70] Haimovici A, Tgliazucchi E, Balenzuela P, Chiavlo D. Brain organization into resting state networks emerges at criticality on a model of the human connectome. Phys Rev Lett 2013;110:178101.
[71] Buldyrev SV, Parshani R, Paul G, Stanley HE, Havlin S. Catastrophic cascade of failures in interdependent networks. Nature 2010;464:1025.
[72] Radicchi F, Arenas A. Abrupt transition in the structural formation of interconnected networks. Nat Phys 2013;9:717.
[73] de Domenico M, Granell C, Porter MA, Arenas A. The physics of multilayer networks. Nat Phys 2016;12:901.
[74] Tononi G, Boly M, Massimini M, Koch C. Integrated information theory: from consciousness to its physical substrate. Nat Rev Neurosci 2016;17:450.
[75] Tononi G. An information integration theory of consciousness. BMC Neurosci 2004;5:42.
[76] Toker D, Sommer FT. Integrated information in large brane networks. arXiv:1708.02967.
[77] Cardy J. Entanglement entropy in extended quantum systems. arXiv:0708.2978.
[78] Friston K. The free-energy principle: a unified brain theory?. Nat Rev Neurosci 2010;11:127.
[79] Krioukov D, Papadopoulos F, Kitsak M, Vahdat A, Boguná M. Hyperbolic geometry of complex networks. Phys Rev E 2010;82:036106.
[80] Ryu S, Takayanagi T. Holographic derivation of entanglement entropy from AdS/CFT. Phys Rev Lett 2006;96:181602.
[81] Brown AR, Roberts DA, Susskind L, Swingle B, Zhao Y. Complexity, action, and black holes. Phys Rev D 2016;93:086006.
[82] Susskind L. Three lectures on complexity and black holes. arXiv:1810.11563 [hep-th].
[83] Mulder D, Bianconi G. Network geometry and complexity. arXiv:1711.06290.
[84] Bianconi G. The entropy of network ensembles. Phys Rev E 2009;79:036114.
[85] Dvali G. Black holes as brains: neural networks with area law entropy. Fortschr Phys 2018;66:040007.
[86] Avetisov V, Gorsky A, Nechaev S, Valba O. Many-body localization and new critical phenomena in regular random graphs and constrained Erdős-Rényi networks. arXiv:1611.08531.